SUPPLEMENTARY MATERIALS

SUPPLEMENTARY METHODS

Cell Culture

4T1 murine breast cancer cells that stably express luciferase (4T1-luc) were cultured in DMEM supplemented with 10% fetal bovine serum. E0771 murine breast cancer cells were cultured in RPMI-1640 with 10% fetal bovine serum (kind gift from Dr. Linda Metheny-Barlow, Wake Forrest University). All cells were harvested by trypsinization at approximately 80% confluence in log phase growth.

Mice

Female BALB/c mice were obtained from Harlan Laboratories, Inc. (Madison, WI) and C57/Bl6 mice were obtained from the National Cancer Institute (Frederick, MD). Tumors were grown orthotopically in the dorsal mammary fat pad following injection of 0.1 mL of DMEM containing 5×10^5 4T1-luc cells in BALB/c mice or 0.2 mL of RPMI-1640 containing 2.5×10^5 E0771 cells in C57/Bl6 mice. Animal care and all experimental procedures were in accordance with the Institutional Animal Care and Use Guidelines at Duke University Medical Center.

Exercise Protocols

Exercise was conducted by voluntary wheel running, which is characterized by intermittent periods of high-intensity, short-duration exercise against low resistance throughout the dark cycle [28]. Mice randomized to exercise groups were given continuous access to an 11.5 cm-diameter wheel (Mini Mitter, Bend, OR), and wheel revolutions were monitored continuously by a magnetic sensor using the VitalView data acquisition program (Respironics, Inc, Murrysville, PA). Mice randomized to sedentary groups were singly housed in cages without wheels.

The exercise intervention was designed to mimic four clinically relevant scenarios: (1) patients who were sedentary before and after diagnosis, (2) previously sedentary patients who begin exercising after diagnosis, (3) physically active patients who stop exercising after diagnosis, and (4) previously active patients who continue to exercise after diagnosis. Mice in Groups 3 and 4 underwent a 9 week pretraining period prior to tumor cell transplant, and mice in Groups 1 and 2 were sedentary during that time. On Day 0 immediately after tumor cell transplant, mice in Groups 2 (SR; sedentary before transplant then running) and 4 (RR; running before and after transplant) were given access to a voluntary running wheel, and mice in Groups 1 (SS; sedentary before and after transplant) and 3 (RS; running before transplantation, then sedentary) were sedentary. The growth rate of tumors in mice in groups 2 and 4 (SR and RR) were identical, as were the growth rates of tumors from groups 1 and 3 (SS and RS). Thus, for statistical analysis, these the SR and RR groups were combined and the SS and RS groups were combined.

Exercise Plus Chemotherapy Protocol

To determine whether exercise affects the efficacy of chemotherapy, BALB/c mice bearing 4T1-luc tumors were randomized to one of four groups: no treatment, exercise alone, cyclophosphamide alone, or exercise plus cyclophosphamide (n=17/group). Mice in exercising groups were given immediate access to a voluntary running wheel. Tumors were allowed to grow for one week, and then mice in the cyclophosphamide groups were injected with the maximally tolerated dose (100 mg/kg) of cyclophosphamide intraperitoneally on Days 7, 9, and 11. Mice in the groups not receiving cyclophosphamide were handled similarly but not injected with chemotherapy. All mice were weighed, tumor volume was measured by calipers, and running data were obtained three times weekly. Additionally, three times weekly, total

hemoglobin and hemoglobin saturation within the tumor were measured using optical spectroscopy as described previously [34]. Prior to euthanasia, three randomly selected mice from each group underwent MR imaging of tumor perfusion as previously described [19]. Three hours prior to sacrifice, all mice received an intraperitoneal injection of 80 mg/kg EF5 [2-2(nitro-1H-imidazole-1-yl)-N-(2,2,3,3,3-pentafluoropropyl acetamide)], a drug that selectively binds to regions of hypoxia (generously provided by Dr. Cameron Koch, University of Pennsylvania, Philadelphia, PA). Tumors were excised when they reached 1500mm^3 or ulcerated, then they were snap-frozen over liquid nitrogen and stored at -80°C.

Immunohistochemistry

Frozen tissue sections (10 μm thick) were stained using specific antibodies as previously described [35]. Briefly, unless otherwise specified, sections were fixed in ice-cold methanol for 30 minutes. Non-specific binding was blocked by a 30-minute incubation at room temperature with 10% donkey serum. Sections were incubated with primary antibodies overnight at 4°C, followed by incubation with the appropriate fluorescently-conjugated secondary antibody. Samples were washed three times for 5 minutes in PBS between each successive step, and all antibodies were diluted in PBS unless otherwise stated. All staining protocols concluded with application of Hoechst 33342 (Sigma Aldrich, St. Louis, MO) for five minutes at room temperature to counterstain for cellular nuclei. Exclusion of the primary antibody served as a negative control. Immunostained slides were stored at 4°C in 4% paraformaldehyde until imaging. Specific staining protocols are described below.

Ki67 and Cleaved Caspase 3. To evaluate apoptosis, slides were stained with anti-cleaved caspase-3 antibody (Cell Signaling Technology, Inc, Danvers, MA), diluted 1:400, followed by incubation with donkey anti-rabbit fluorescent secondary antibody (DyLight 594,

Jackson), diluted 1: 1,000. To evaluate tumor cell proliferation, sections were fixed with 4% paraformaldehyde, permeabilized with 0.5% saponin, and incubated overnight with rat anti-Ki67 (Dako North America, Inc, Carpinteria, CA), followed by incubation with donkey anti-rat fluorescent secondary antibody diluted 1:1000 (DyLight 488, Jackson). All washes and antibody dilutions were performed with 0.5% saponin in PBS.

CD31, Desmin, and NG2. To stain for vasculature, sections were incubated for 1 hour with rat anti-mouse CD31 antibody (BD Pharmingen, San Diego, CA), diluted 1:100, followed by incubation with donkey anti-rat fluorescent secondary antibody (DyLight 488, Jackson ImmunoResearch Laboratories, Inc, West Grove, PA), diluted 1: 1,000. Pericyte coverage was assessed by desmin co-localization with CD31, and this was confirmed with NG2 co-localization with CD31. For NG2 staining, slides were fixed in a 1:1 mix of acetone and methanol. Following fixation and blocking, slides were treated with rabbit polyclonal anti-Desmin (Abcam, Cambridge, MA), diluted 1:200 or rabbit polyclonal anti-NG2 (Millipore, Billerica, MA), diluted 1:400 overnight, followed by incubation with donkey anti-rabbit fluorescent secondary antibody (DyLight 594, Jackson), diluted 1: 1,000.

EF5. The hypoxia marker EF5 was detected using a Cy5-conjugated mouse monoclonal ELK3-51 antibody (purchased from Dr. Cameron Koch, University of Pennsylvania) applied 1:2 overnight at 4°C.

Microscopy and Image Analysis

Slides were imaged using a high-resolution solid-state camera mounted on a fluorescence microscope (Axioscop Zplus, Carl Zeiss, Inc., Thornwood, NY). A 4′,6-diamidino-2-phenylindole filter was used to detect Hoechst 33342. CD31, Ki67, and cleaved caspase-3 staining were detected with a FITC filter. NG2 and desmin staining were detected with a TRITC

filter. EF5 images were detected with a Cy5 filter. All images were captured at 5x magnification in 16-bit monochrome signal depth. Fixed exposure times were preselected for each fluorochrome. A computer-controlled motorized stepping stage (Metamorph Imagining System, Molecular Devices Corporation, Sunnyvale, CA) was used to tile individual fields and stitch them to generate composite images of every tissue section.

The nuclear counterstain permitted region of interest (ROI) contour lines to be drawn around each tumor, and necrotic regions were excluded from ROIs based on the absence of tumor cell nuclei. Microvessel density (MVD) was calculated for each section by overlaying a fixed grid on the CD31 image (Adobe Photoshop CS2, Adobe Systems, Inc., San Jose, CA). Individual CD31-positive vessels were manually counted in every other visible field to determine a mean value for the section. All other immunostains were analyzed using Image J software (NIH, http://rsb.info.nih.gov/ij/). First, a single optimal threshold value was set for each channel on every set of images. All images in a series were analyzed using the same threshold to determine positively stained pixels within the ROI. For the nuclear stains Ki67 and cleaved caspase-3, positive cells were counted from thresholded images using the particle analysis tool. To analyze pericyte coverage of tumor vessels, thresholded desmin images were overlaid on thresholded CD31 images. This procedure was repeated for NG2 colocalization with CD31. The total tumor area fraction containing colocalized pixels and the CD31-positive area fraction containing colocalized vessels were calculated to determine the fraction of tumor area containing mature blood vessels and vessel area covered by pericytes, respectively. Hypoxic tumor fraction was assessed by determining the amount of EF5-positively stained area divided by the total tumor area. Images were colored and adjusted for brightness and contrast for presentation only.

Angiogenesis Gene Expression

Total RNA was extracted from the 4T1 tumors using the Qiagen RNeasy Miniprep Kit (Qiagen, Inc, Valencia, CA) according to the manufacturer's instructions. Approximately 1 μg of RNA was reverse-transcribed using the Bio-Rad iScript cDNA Synthesis Kit (Bio-Rad Laboratories, Inc, Hercules, CA), and resulting cDNA was stored at -20°C until analysis. Quantitative Real-Time PCR (QPCR) was performed using iQ SYBRGreen Supermix (Bio-Rad) according to the manufacturer's instructions. Gene expression was quantified ($2^{-\Delta\Delta Ct}$) relative to the RPL19 housekeeping gene. The primers and PCR conditions are described in Supplementary Table 1.

Western Blotting of Tumor Samples

A sample (approximately 500 μg) was cut from each frozen tumor and dounce homogenized in lysis buffer (25 mM TRIS (pH 7.5), 150 mM sodium chloride, 2 mM EDTA, 1 mM dithiothreitol, 1% Triton X-100, 1% protease inhibitor cocktail (Roche Diagnostics Co, Indianapolis, IN), and 1X phosphatase inhibitor (Halt, Thermo Fisher Scientific, Inc., Waltham, MA). Following a clarification spin, protein concentrations of the lysates were determined by BioRad assay and normalized. Fifty μg of protein lysate was loaded per lane of denaturing gel (Bio-Rad Laboratories, Hercules, CA) and subsequently transferred to PVDF membrane (Immobilon-P) for Western blotting. Primary antibodies were used as per manufacturer's instructions, and secondary antibodies were used at 1:10000 dilution. The sources of primary antibodies are as follows: XIAP (BD Biosciences); Caspase 8, PARP, and Fas (Cell Signaling Technology); Bcl-2 (Santa Cruz Biotechnology); and PDGFR-β (Novus Biologicals, Littleton, CO). Proteins were visualized by enhanced chemoluminescence (Pierce, Thermo Fisher Scientific) on autoradiography film. Quantification of bands was performed by Image J software and statistically analyzed.

MRI Perfusion Imaging

On the last day of the experiment, mice in the 4T1 experiment underwent MR imaging (n = 3 per group) to determine tumor perfusion using a Bruker 7T (70/30) system (Bruker Biospin, Billerica, MA, USA). This system has a quadrature surface receiver and volume transmit coil setup with active decoupling. Mice were anesthetized with isoflurane and positioned in an MR-compatible cradle that maintains body temperature using warm water circulation. Temperature and respiratory rate were continuously monitored. First, anatomic information was acquired by T2-weighted imaging using a RARE-based fast spin echo sequence with TR=4200, TE=12, RARE factor 8, 1 mm slice thickness, FOV 2.4 cm, 256 x 256, with respiratory gating. Tumor perfusion maps were generated by a double spin-echo planar pulse sequence using pairs of bipolar gradients at specific predetermined signs in each of three orthogonal directions. The combination of gradient directions allows cancellation of all off‐ diagonal tensor elements, hence measurement of the diffusion tensor trace, and so provides unambiguous and rotationally invariant apparent diffusion coefficient (ADC) values. Seven *b* values (b = 0, 50.0, 100, 150, 200, 500, 1000) were acquired, with a matrix size of 128 x 128, slice thickness 1.0 mm. Volume images (one for each *b* value) were created from raw DICOM images. For voxels within the 128Å~128Å~15 matrix with a signal value above 2000, the ADC at each voxel was calculated using an exponential moving fit by the following method: ADC = ln [S(*b = b1*) – S(*b = b2*)/*b2-b1*. The *b1* and *b2* values of 100 and 200, respectively, are sensitive to blood flow apparent diffusion changes in small arteries

and capillaries. ADC maps were generated using mono-exponential fitting as above, and T2 images were zero-filled to 256Å~256 prior to analysis. Parametric images were analyzed in anatomic regions of interest using Bruker Paravision software and offline using Osirix software.

Statistical Analyses

Statistical analysis was carried out using StatView 5.0.1 (SAS Institute, Inc, Cary, NC) and JMP Pro 11 (SAS Institute, Inc, Cary, NC). Descriptive statistics are presented as mean ± 95% CI. One-way ANOVA was used to compare differences in tumor variables between groups. Repeated measures ANOVA was used to compare differences in body weight and running distance between groups throughout the experiments. All ANOVA and repeated measure ANOVA tests were followed by Fisher's protected least significant difference to determine whether individual groups differed from the control group if the data were normally distributed or the Mann-Whitney U test for data that were not normally distributed. Tumor growth rates were determined by linear regressions, and differences in growth rate between groups were assessed using an ANCOVA. For all tests, $p<0.05$ was considered statistically significant and all t-tests are expressed as two sided tests.

Supplementary Table 1: Summary of PCR Protocols

Gene of Interest	Forward Primer	Reverse Primer	Thermocycle Conditions
RPL19	5'-ATCCGCAAGCCTGTGACTGT-3'	5'-TCGGGCCAGGGTGTTTTT-3'	
VEGF	5'-CTGTGCAGGCTGCTGTAACG-3'	5'-GTTCCCGAAACCCTGAGGAG-3'	• Denaturation: 95°C for 10 min • 30 cycles: denaturation at 94°C for 30 sec, annealing at 56°C for 30 sec, elongation at 72°C for 30 sec • Dissociation 95°C for 15 sec, 60°C for 15 sec, 95°C for 15 sec

Supplementary Figure 1. E0771 tumor response to exercise. Tumor growth rate is statistically significantly slowed by exercise. Data are expressed as means; error bars are 95%CI, p=0.012, ANCOVA.

Supplementary Figure 1

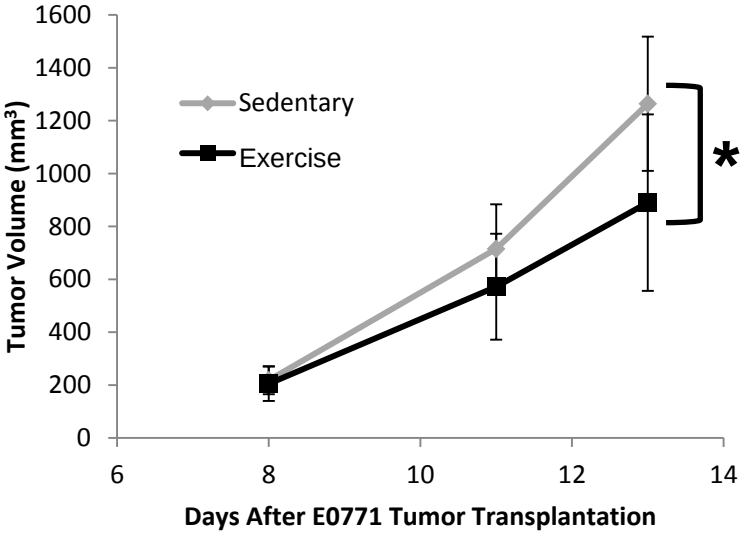

Supplementary Figure 2. Left panel: Body weights over time of BALB/c mice randomized to exercise or sedentary control. Body weights increased over time in both the exercise and sedentary groups, but there were no statistically significant differences between treatment groups at any time point. Data are expressed as means; error bars are 95%CI, two-sided t-test. **Right panel:** Body weights over time of C57Bl/6 mice randomized to voluntary wheel running or sedentary control. Body weights did not change notably over the course of the experiment in either group, and there were no statistically significant differences between treatment groups at any time point. Data are expressed as means; error bars are 95% CI, two-sided t-test.

Supplementary Figure 2

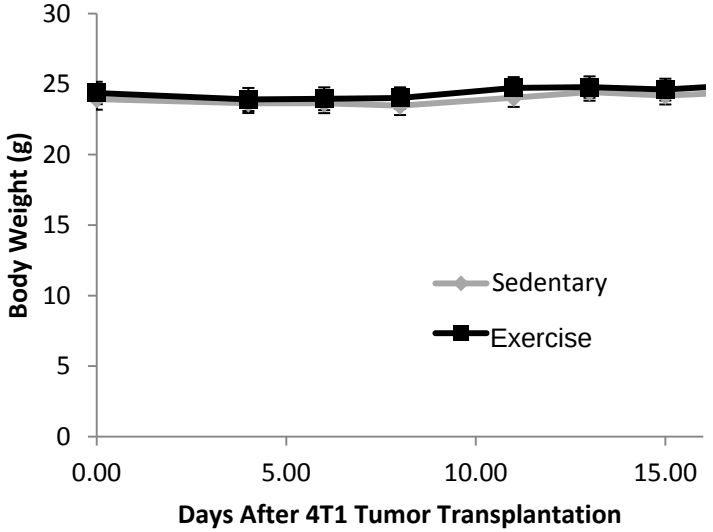

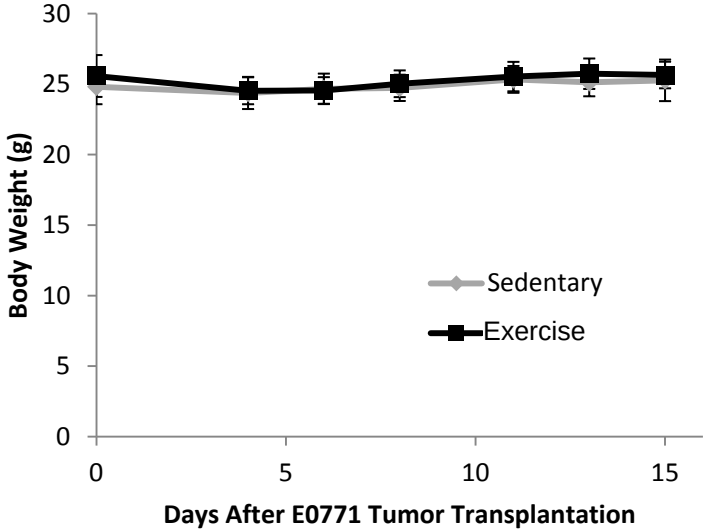

Supplementary Figure 3. Effects of exercise on angiogenesis in primary E0771 breast tumors. Immunostaining for blood vessels shows that microvessel density (CD31) was statistically significantly higher in the tumors from exercising animals compared to sedentary controls. Scatter points, individual animals; gray lines, mean; black lines, 95%CI, p=0.010, two-sided t-test.

Supplementary Figure 3

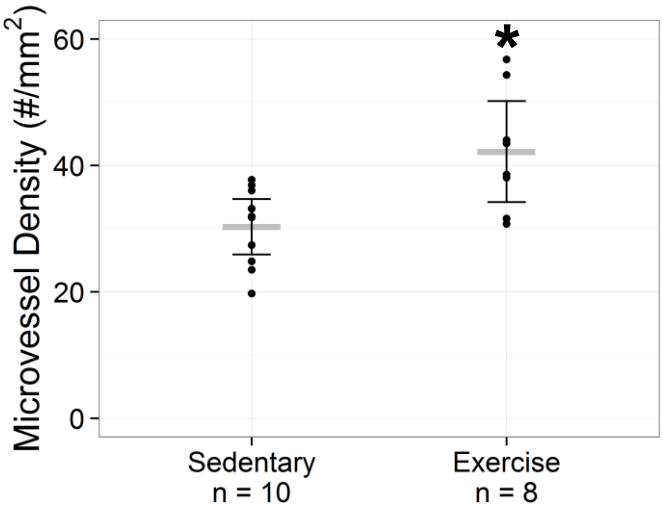

Supplementary Figure 4. Effects of exercise on expression of VEGF and PDGFR-β in tumor tissue. **A**. Total RNA was extracted from 4T1-luc tumors and reverse transcribed. Gene expression was quantified relative to the RPL19 housekeeping gene. Each sample was run in triplicate. Tumors from exercising animals had statistically significantly higher expression of VEGF mRNA than sedentary controls. Scatter points, individual animals; gray lines, mean; black lines, 95%CI; p=0.011, two-sided t-test. B. Protein was extracted from 4T1-luc tumors and expression levels of PDGFR-β were visualized on western blots. Band intensity was quantified in comparison to actin loading controls. PDGFR-β expression was statistically significantly lower in tumors from exercised mice, p=0.013, two-sided t-test.

Supplementary Figure 4

A

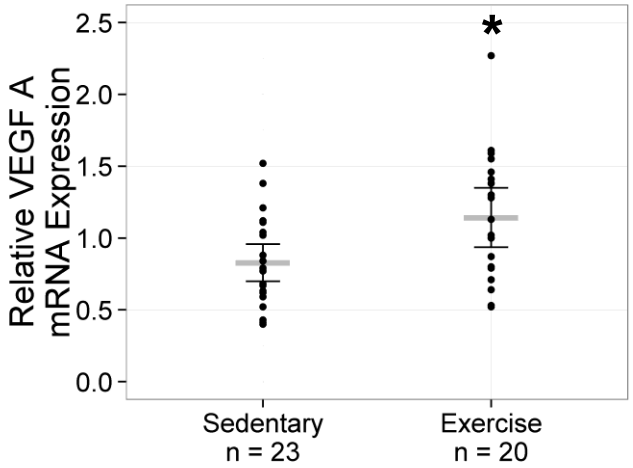

B

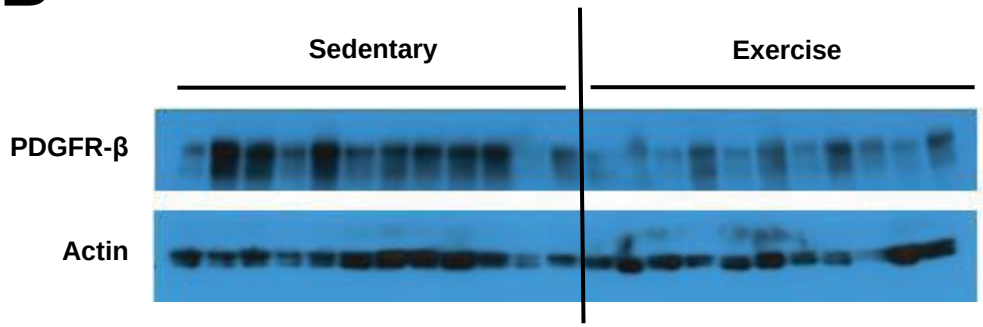

	Fold change (R/S)	Rank sum
PDGFR-β	0.6333	0.0134

Supplementary Figure 5. Effects of exercise on tumor perfusion. Animals from both exercise and sedentary treatment groups (n=6/group) bearing 4T1-luc tumors in the mammary fat pad underwent in vivo MR perfusion mapping. Mean ADC_{perf} was calculated for each tumor, and patterns of perfusion were analyzed qualitatively. ADC is the Apparent Diffusion Coefficient of water, which is a method of MRI data acquisition that detects blood flow in small arterioles and capillaries without requiring a contrast agent. Tumors from sedentary animals (**A**) showed highly heterogeneous patterns of flow, with more perfusion around the edges of the tumor and less in the center. In comparison, tumors from exercising animals (**B**) were more uniformly perfused. (C) Overlaid shadow histograms showing the distribution of perfusion values in exercising and sedentary animals. (D) Bar chart showing the variability of perfusion values in the tumor (region of interest, ROI) in exercising versus sedentary animals. (E) Overlaid shadow histograms showing the distribution of perfusion values in exercising and sedentary C57/Bl6 animals bearing E0771 tumors. The mean tumor perfusion in the exercising animals was statistically significantly higher than that of sedentary animals, *$p<0.001$, Student's *t*-test.

Supplementary Figure 5